Communication

Synthesis and Characterization of Ordered Intermetallic PtPb Nanorods

Sean Maksimuk, Shengchun Yang, Zhenmeng Peng, and Hong Yang

J. Am. Chem. Soc., **2007**, 129 (28), 8684-8685• DOI: 10.1021/ja071980r • Publication Date (Web): 20 June 2007

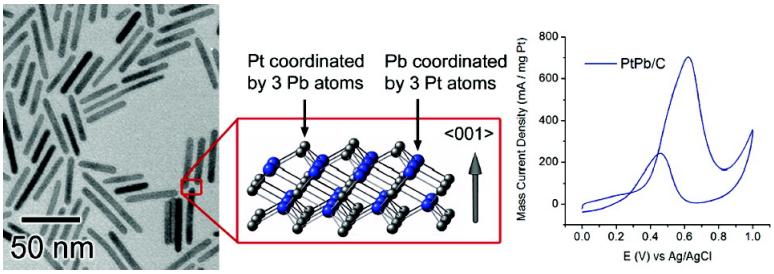

More About This Article

Additional resources and features associated with this article are available within the HTML version:

- Supporting Information
- Links to the 12 articles that cite this article, as of the time of this article download
- Access to high resolution figures
- Links to articles and content related to this article
- Copyright permission to reproduce figures and/or text from this article

View the Full Text HTML

J|A|C|S
COMMUNICATIONS

Published on Web 06/20/2007

Synthesis and Characterization of Ordered Intermetallic PtPb Nanorods

Sean Maksimuk, Shengchun Yang, Zhenmeng Peng, and Hong Yang*

Department of Chemical Engineering, University of Rochester, 206 Gavett Hall, Rochester, New York 14627

Received March 20, 2007; E-mail: hongyang@che.rochester.edu

Intermetallics are compounds of metals that display crystal structures different from the constituent metals.[1] Consequently, these materials possess distinctly different electronic, magnetic, catalytic, and mechanical properties in comparison to their disordered alloy counterparts. In recent years, crystal phase- and shape-controlled platinum-based intermetallic nanostructures have attracted lots of research attention because of their potential applications in ultrahigh magnetic data storage as illustrated in face-centered tetragonal (fct) FePt nanoparticles.[2−4] Furthermore, it has recently been identified that platinum-containing intermetallic phases such as PtPb, PtBi, and PtIn show superior electrocatalytic properties toward the oxidation of small organic molecules for fuel cell applications when compared to their disordered alloys.[5]

The nonhydrolytic colloidal synthesis of nanoparticles has garnered the attention of many researchers because of its versatility and success in synthesizing nanoparticles of various compositions and shapes.[6−9] The colloidal intermetallic nanoparticles can be synthesized either by co-reduction of metal cations[10,11] or mixing a known amount of metal nanoparticles followed by an annealing process.[12−14] In either case the final products were composed of large aggregates of nanoparticles, which are not desirable for catalytic application. The control of size and shape of intermetallic nanoparticles, however, has been met with limited success because of the difficulty in achieving the simultaneous reduction of cationic metal precursors and the inability to identify suitable stabilizing agents. The intrinsic crystal structures possessed by intermetallics, however, should promote the formation of nanoparticles with interesting shapes. In this Communication, we demonstrate the synthesis of ordered intermetallic PtPb nanorods. The formation of rodlike morphology is attributed to the difference in coordination numbers of the platinum or lead adatoms of the growing low-index surfaces.

PtPb nanorods were synthesized by simultaneously reducing platinum acetylacetonate ($Pt(acac)_2$) and lead acetylacetonate ($Pb(acac)_2$) with *tert*-butylamine−borane (TBAB) complex in a mixture of diphenyl ether, adamantanecarboxylic acid (ACA), hexadecanethiol (HDT), and hexadecylamine (HDA) at 180 °C under an inert atmosphere.[15] Figure 1 shows the transmission electron microscopy (TEM) images, selected area electron diffraction (SAED), and powder X-ray diffraction (PXRD) patterns of the PtPb nanorods made at a reaction time of 30 min. These nanorods had an average length of 45 ± 12 nm and a width of 5.9 ± 3.4 nm, which led to an average aspect ratio of 8.2 ± 2.8 (Figure 1a and Figure S1). The inset of Figure 1a is a high-resolution TEM image of the tip of a representative nanorod. The lattice distance normal to the growth direction of the rods was 2.76 Å, matching that of PtPb (002) plane. The lattice plane parallel to the long-axis of the nanorod had a *d*-spacing of 2.12 Å and could be assigned to the (110) plane. The SAED diffraction pattern of a single nanorod matched that of the simulated electron diffraction (ED) pattern of an intermetallic PtPb single crystal viewed along the ⟨110⟩ zone axis shown in the inset of Figure 1b.[16,17] The observed *d*-spacings

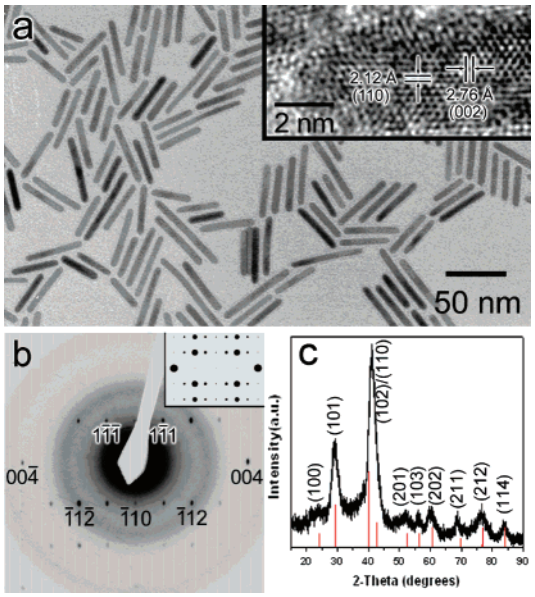

Figure 1. (a) TEM image and (b) selected area electron diffraction pattern from a single PtPb nanorod and (c) PXRD pattern of ensemble of PtPb nanorods. The inset of panel a shows a HRTEM image of the tip region of a PtPb nanorod. The inset of panel b shows a simulated electron diffraction pattern from a single PtPb nanorod with the ⟨110⟩ zone axis.

calculated from the SAED pattern were consistent with those of the hexagonal PtPb with $a = 5.48$ Å and $c = 4.24$ Å (space group: $P6_3/mmc$), which has the NiAs-type structure, Table S1. The elliptical shape of the diffraction spots arise because of an anisotropic distribution of shape factors of the PtPb nanorods,[18] where the short axis of the diffraction spot was parallel to the (001) directions, confirming that the nanorods grew along the *c*-axis. The PXRD pattern confirms the nanorods were made of pure PtPb intermetallic phase (JCPDS database-International Centre for Diffraction Data, 1999, PCPDFWIN version 2.02) (Figure 1c). The energy-dispersive X-ray (EDX) spectroscopy data also indicate that the Pt/Pb atomic ratio was ∼50/50 for as-synthesized nanorods, Figure S2.

In this reaction mixture, the Pt^{2+} and Pb^{2+} salts were reduced to intermetallic PtPb by a strong reducing agent, TBAB.[19] While TBAB was very important in the shape control, the molar ratios and reaction time of other reagents, including HDA, ACA, and HDT, were also critical for obtaining PtPb intermetallic nanorods (Figures S3−S6). This result was in contrast to those previously synthesized PtPb nanoparticles, where irregular aggregates formed.[10,11]

The formation of rodlike morphology could be explained by the difference in the numbers of coordination sites along various low-index surfaces of the hexagonal crystal structure of PtPb. Figure 2a shows the hexagonal cell of PtPb viewed from ⟨00−1⟩ direction. There existed two low-index equivalent directions perpendicular to the unique *c*-axis: the [−110] directions which also included the ⟨−1−20⟩ direction and [100] directions which included ⟨110⟩

10.1021/ja071980r CCC: $37.00

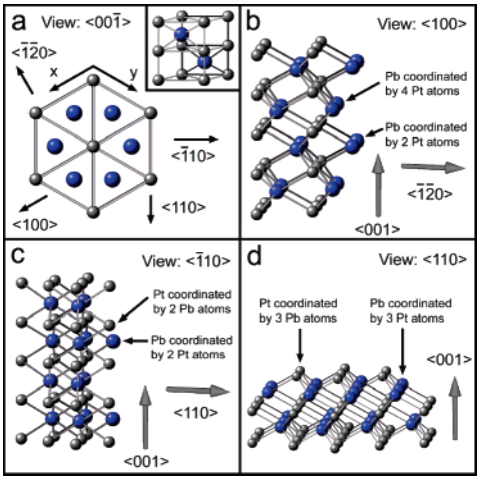

Figure 2. (a) The PtPb crystal structure and (b−d) the growing surfaces viewed along (a) ⟨00−1⟩, (b) ⟨100⟩, (c) ⟨−110⟩, and (d) ⟨110⟩ directions, respectively. Inset of panel a is the unit cell of intermetallic PtPb. Only the growth along [001] directions involved 3-fold sites, while those along [110] or [100] directions involved at least one type of 2-fold binding sites. The viewing directions of panels b−d were slightly offset for clarity. The gray and blue balls represent Pt and Pb atoms, respectively.

direction. Careful crystallographic examination reveals that crystal growth perpendicular to the *c*-axis is unfavorable because of relatively low numbers of binding sites for adatom incorporation. For a Kossel crystal, adatom preferably incorporates into a site with a high-coordination number because of the strong binding energy, which is proportional to the number of nearest neighbors.[20] Growth in the ⟨−1−20⟩ direction of intermetallic PtPb involved two types of lead adatom sites: one in which the adsorbed lead atom is coordinated by four platinum atoms and the other by two platinum atoms, Figure 2b. The lead atom coordinated by two platinum atoms was unstable and growth in the equivalent [−1−20] directions was limited. Growth in the ⟨110⟩ direction involved sites where the platinum atom was coordinated by two lead atoms and vice versa, suggesting that growth in the equivalent [110] directions is also unfavorable (Figure 2c). Growth in the [001] directions, however, involved 3-fold coordinated sites for both platinum and lead adatoms. The relatively high-binding numbers for both types of adatoms mean the favorable sites for adatom incorporation are along [001] directions, that is, the unique *c*-axis.

The electrocatalytic properties of PtPb intermetallic nanostructure toward the methanol oxidation reaction were tested. The PtPb nanorods were deposited onto carbon black (Vulcan XC-72) and treated in air plasma before further annealing at 600 °C for 2 h under an atmosphere of 5% (v/v) H_2 in argon. This treatment led to the change in morphology (Figure S7). Figure 3 shows the cyclic voltammogram recorded at a scan rate of 50 mV s^{-1} after 50 cycles.[15] The peak mass current density was above 700 mA mg^{-1} Pt. This value was significantly higher than that of a commercial PtRu/C catalyst (Johnson-Matthey, 30 wt % Pt and 15 wt % Ru) when normalized to the unit mass of platinum.

In conclusion, we demonstrated a synthesis of ordered intermetallic PtPb nanorods. The formation of rodlike morphology is attributed to the adatom incorporation onto the growing surfaces with strong binding sites for both Pt and Pb atoms along low-index

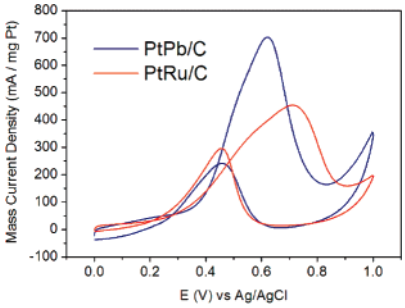

Figure 3. Cyclic voltammograms of electrocatalytic oxidation of methanol with PtPb/C and a commercial PtRu/C catalyst.

directions. The synthetic strategy should open up new avenues to the simultaneous composition and shape control of ordered intermetallic nanoparticles.

Acknowledgment. This work was supported by a NSF CAREER Award (Grant DMR-0449849). It made use of the FEI Tecnai F-20 microscope at Cornell Center for Materials Research (CCMR) funded in part by NSF (Grant DMR-0520404). S.C.Y. is a visiting student from Jiatong University. We thank John Grazul for help in running the HR-TEM.

Supporting Information Available: Synthesis and characterization of PtPb nanorods (TEM images, EDX data, ED analysis, PXRD data, and simulation, Figures S1−S7 and Table S1). This material is available free of charge via the Internet at http://pubs.acs.org.

References

(1) Sauthoff, G. *Intermetallics*; VCH: Weinheim, Germany, 1995.
(2) Jeong, U.; Teng, X. W.; Wang, Y.; Yang, H.; Xia, Y. N. *Adv. Mater.* **2007**, *19*, 33−60.
(3) (a) Sun, S. H. *Adv. Mater.* **2006**, *18*, 393−403. (b) Sun, S. H.; Murray, C. B.; Weller, D.; Folks, L.; Moser, A. *Science* **2000**, *287*, 1989−1992.
(4) Lu, A.-H.; Salabas, E. L.; Schüth, F. *Angew. Chem., Int. Ed.* **2007**, *46*, 1222−1244.
(5) Casado-Rivera, E.; Volpe, D. J.; Alden, L.; Lind, C.; Downie, C.; Vazquez-Alvarez, T.; Angelo, A. C. D.; DiSalvo, F. J.; Abruna, H. D. *J. Am. Chem. Soc.* **2004**, *126*, 4043−4049.
(6) Wiley, B.; Im, S.-H.; Li, Z.-Y.; McLellan, J. M.; Siekkinen, A.; Xia, Y. *J. Phys. Chem. B* **2006**, *110*, 15666−15675.
(7) Yin, Y.; Alivisatos, A. P. *Nature* **2005**, *437*, 664−670.
(8) Xia, Y. N.; Yang, P. D.; Sun, Y. G.; Wu, Y. Y.; Mayers, B.; Gates, B.; Yin, Y. D.; Kim, F.; Yan, Y. Q. *Adv. Mater.* **2003**, *15*, 353−389.
(9) (a) Jun, Y. W.; Choi, J. S.; Cheon, J. *Angew. Chem., Int. Ed.* **2006**, *45*, 3414−3439. (b) Jun, Y. W.; Lee, J. H.; Choi, J. S.; Cheon, J. *J. Phys. Chem. B* **2005**, *109*, 14795−14806.
(10) Roychowdhury, C.; Matsumoto, F.; Zeldovich, V. B.; Warren, S. C.; Mutolo, P. F.; Ballesteros, M.; Wiesner, U.; Abruna, H. D.; DiSalvo, F. J. *Chem. Mater.* **2006**, *18*, 3365−3372.
(11) Alden, L. R.; Roychowdhury, C.; Matsumoto, F.; Han, D. K.; Zeldovich, V. B.; Abruna, H. D.; DiSalvo, F. J. *Langmuir* **2006**, *22*, 10465−10471.
(12) Cable, R. E.; Schaak, R. E. *Chem. Mater.* **2005**, *17*, 6835−6841.
(13) Schaak, R. E.; Sra, A. K.; Leonard, B. M.; Cable, R. E.; Bauer, J. C.; Han, Y. F.; Means, J.; Teizer, W.; Vasquez, Y.; Funck, E. S. *J. Am. Chem. Soc.* **2005**, *127*, 3506−3515.
(14) Cable, R. E.; Schaak, R. E. *J. Am. Chem. Soc.* **2006**, *128*, 9588−9589.
(15) See Supporting Information for details.
(16) Weber, S. JSV1.08lite. http://jcrystal.com/steffenweber/JAVA/JSV/jsv.html, 1999.
(17) The radius of the spots of the simulated electron diffraction pattern is relative to the structure factor *F* multiplied by its complex conjugate *F**, *i.e.*: *F*F*.
(18) Fultz, B.; Howe, J. *Transmission Electron Microscopy and Diffractometry of Materials*; Springer: Berlin, 2001.
(19) Zheng, N.; Fan, J.; Stucky, G. D. *J. Am. Chem. Soc.* **2006**, *128*, 6550−6551.
(20) Mutaftschiev, B. *The Atomistic Nature of Crystal Growth*; Springer: Berlin, 2001.

JA071980R